

Competitive Bimolecular Electron- and Energy-Transfer Quenching of the Excited State(s) of the Tetranuclear Copper(I) Cluster $\text{Cu}_4\text{I}_4\text{py}_4$. Evidence for Large Reorganization Energies in an Excited-State Electron Transfer

Anders Døssing,^{1a} Chong Kul Ryu, Setsuko Kudo,^{1b} and Peter C. Ford*

Contribution from the Department of Chemistry, University of California, Santa Barbara, California 93106

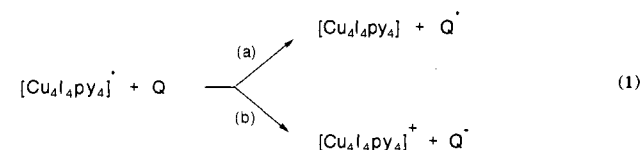
Received September 10, 1992

Abstract: The quenching of emission from the cluster-centered (ds/XMCT) excited state of the copper(I) cluster $\text{Cu}_4\text{I}_4\text{py}_4$ (I, py = pyridine) by tris(β -dionato)chromium(III) complexes CrL_3 and several organic substrates has been investigated in dichloromethane solution. The E^0 energy of the excited state (I^*) was estimated to be $1.66 \mu\text{m}^{-1}$ (2.06 V), and the reduction potential $E_{1/2}(\text{I}^+/\text{I}^*)$ was estimated as -1.78 V (vs the ferrocenium/ferrocene couple). Each of the CrL_3 complexes (${}^2E_g \sim 1.3 \mu\text{M}^{-1}$) is capable of energy transfer quenching, and the rate of this process is shown to be about $10^{7.9} \text{ M}^{-1} \text{ s}^{-1}$. Contributions to the quenching by an apparent electron-transfer mechanism were evident for those substrates with reduction potentials $E_{1/2}(\text{Q}/\text{Q}^-)$ less than 1.4 V, i.e. reaction driving forces ($-\Delta G_{\text{el}}^0$) greater than 0.4 V. The large driving force required can be attributed to a very slow I^+/I^* self-exchange rate and is indicative of large contributions from inner sphere terms to the total electron-transfer reorganization energy. Such contributions are a likely explanation of the substantially positive ΔH_q^* values (up to +40 kJ mol⁻¹) noted for organic quenchers with $E_{1/2}(\text{Q}/\text{Q}^-)$ near 1.4 V. Pressure effect studies demonstrate that the activation volume (ΔV_q^*) for energy-transfer quenching of the CrL_3 species is $\sim 0 \text{ cm}^3 \text{ mol}^{-1}$ while that of those quenchers which operate near the diffusion limit is $\sim +7 \text{ cm}^3 \text{ mol}^{-1}$, consistent with the expected effects on solvent viscosity. In contrast, for those systems with $E_{1/2}(\text{Q}/\text{Q}^-) \sim 1.4 \text{ V}$, substantially negative ΔV_q^* values were observed, a feature reflective of the solvent reorganization owing to charge creation upon electron transfer between I^* and Q.

Introduction

The rich photoluminescence properties of polynuclear complexes of transition metals having the d^{10} electronic configuration have been amply demonstrated in this laboratory and others.²⁻¹² For example, the ambient-temperature, solution-phase lumines-

cence spectrum of the tetranuclear copper(I) cluster $\text{Cu}_4\text{I}_4\text{py}_4$ (I, py = pyridine) is dominated by an intense ($\lambda_{\text{max}}^{\text{em}} \sim 690 \text{ nm}$), long-lived ($\tau = 3\text{--}10 \mu\text{s}$ in different solvents) emission from an excited state (ES) assigned as "cluster centered" (CC) with mixed iodide-to-copper charge transfer (XMCT) and d-s character.^{2a,c} Such a long lifetime offers the possibility of harvesting the excitation energy via bimolecular processes. The present investigation was initiated to examine possible roles of competitive bimolecular quenching of the excited states of such copper(I) clusters in solution.



The quenchers described here include a series of uncharged tris(β -dionato)chromium(III) complexes¹³ CrL_3 and several organic oxidants. The CrL_3 complexes display a remarkably wide range of reduction potentials (-2.43 to -0.79 V vs ferrocenium/ferrocene, Fc^+/Fc , in CH_2Cl_2 solution)¹⁴ but have relatively invariant 2E_g ligand field ES energies ($1.22\text{--}1.28 \mu\text{m}^{-1}$).¹⁵ These have been shown to quench the luminescence of the

(12) Henary, M.; Zink, J. I. *J. Am. Chem. Soc.* **1989**, *111*, 7407–7411; *Inorg. Chem.* **1991**, *30*, 3111–3112.

(13) For the various CrL_3 ligand abbreviations are acac, 2,4-pentanedionate; 3-Br-acac, 3-bromo-2,4-pentanedionate; dbm, 1,3-diphenyl-1,3-pentanedionate; 3-SCNacac, 3-thiocyanato-2,4-pentanedionate; tfac, 1,1,1-trifluoro-2,4-pentanedionate; 3-NO₂acac, 3-nitro-2,4-pentanedionate; tta, thenoyltrifluoroacetate; tfbzac, 4,4,4-trifluoro-1-phenyl-1,3-butanedionate; hfac, 1,1,1,5,5,5-hexafluoro-2,4-pentanedionate.

(14) Gamache, R. E., Jr.; Rader, R. A.; McMillin, D. R. *J. Am. Chem. Soc.* **1985**, *107*, 1141–1146.

(15) Fatta, A. M.; Lintvedt, R. L. *Inorg. Chem.* **1971**, *10*, 478–481.

(1) (a) Danish Natural Science Foundation Postdoctoral Fellow, 1991. (b) Visitor from Institute for Advanced Materials Processing, Tohoku University, Sendai 980, Japan.

(2) (a) Kyle, K. R.; Ryu, C. K.; DiBenedetto, J. A.; Ford, P. C. *J. Am. Chem. Soc.* **1991**, *113*, 2954–2965. (b) Kyle, K. R.; Ford, P. C. *J. Am. Chem. Soc.* **1989**, *111*, 5005–5006. (c) Ryu, C. K.; Kyle, K. R.; Ford, P. C. *Inorg. Chem.* **1991**, *30*, 3982–3986. (d) Vitale, M.; Palke, W. E.; Ford, P. C. *J. Phys. Chem.* **1992**, *96*, 8329–8336. (e) Sabin, F.; Ryu, C. K.; Vogler, A.; Ford, P. C. *Inorg. Chem.* **1992**, *31*, 1941–1945. (f) Ryu, C. K.; Vitale, M.; Ford, P. C. *Inorg. Chem.* **1993**, *32*, 862–874. (g) Ford, P. C.; Vogler, A. *Acc. Chem. Res.*, in press.

(3) (a) Crosby, G. A.; Highland, R. G.; Truesdell, K. A. *Coord. Chem. Rev.* **1985**, *64*, 41–53. (b) Parker, W. L.; Crosby, G. A. *J. Phys. Chem.* **1989**, *93*, 5692–5696.

(4) Kutal, C. *Coord. Chem. Rev.* **1990**, *99*, 213–252.

(5) Harvey, P. D.; Gray, H. B. *J. Am. Chem. Soc.* **1988**, *110*, 2145–2147.

(6) (a) Balch, A. L.; Nagle, J. K.; Oram, D. E.; Reedy, P. E., Jr. *J. Am. Chem. Soc.* **1988**, *110*, 454–462. (b) Balch, A. L.; Catalano, V. J.; Olmstead, M. M. *J. Am. Chem. Soc.* **1990**, *112*, 2010–2011.

(7) King, C.; Wang, J.-C.; Khan, M. N. I.; Fackler, J. P., Jr. *Inorg. Chem.* **1989**, *28*, 2145–2149.

(8) (a) McMillin, D. R.; Kirchoff, J. R.; Goodwin, K. V. *Coord. Chem. Rev.* **1985**, *64*, 83–92. (b) Ichinaga, A. K.; Kirchoff, J. R.; McMillin, D. R.; Dietrich-Buchecker, C. O.; Marnot, P. A.; Sauvage, J.-P. *Inorg. Chem.* **1987**, *26*, 4290–4292. (c) Crane, D. R.; DiBenedetto, J.; Palmer, C. E. A.; McMillin, D.; Ford, P. C. *Inorg. Chem.* **1988**, *27*, 3698–3700. (d) Casandonte, D. J.; McMillin, D. R. *J. Am. Chem. Soc.* **1987**, *109*, 331–337. (e) Stacy, E. M.; McMillin, D. R. *Inorg. Chem.* **1990**, *29*, 393–396.

(9) Stillman, M. J.; Zelazowski, A. J.; Szymanska, J.; Gasyina, Z. *Inorg. Chim. Acta* **1989**, *161*, 275–279.

(10) (a) Rath, N. P.; Holt, E. M.; Tanimura, K. *Inorg. Chem.* **1985**, *24*, 3934–3938. (b) Rath, N. P.; Maxwell, J.; Holt, E. M. *J. Chem. Soc., Dalton Trans.* **1986**, 2449–2453. (c) Tompkins, J. A.; Maxwell, J. L.; Holt, E. M. *Inorg. Chim. Acta* **1987**, *127*, 1–7.

(11) (a) Vogler, A.; Kunkely, H. *J. Am. Chem. Soc.* **1986**, *108*, 7211–7212. (b) Vogler, A.; Kunkely, H. *Chem. Phys. Lett.* **1989**, *158*, 74–76. (c) Kunkely, H.; Vogler, A. *J. Chem. Soc., Chem. Commun.* **1990**, 1204–1205.

mononuclear complex $\text{Cu}(\text{dpp})_2^+$ (dpp = 2,9-diphenylphenanthroline) by competitive energy and electron-transfer mechanisms.^{14,16} The organic quenchers each have lowest ES energies above the estimated E^{00} for $\text{I}^* 2a$ (thus, energy transfer is not likely), while their reduction potentials span a $E_{1/2}(\text{Q}/\text{Q}^-)$ range of -1.37 to -0.94 V (vs Fc^+/Fc in CH_2Cl_2).

Experimental Section

Materials. The Cu_4Ipy_4 was prepared as described^{2a} then recrystallized twice from benzene/hexane. The tris(β -dionato)chromium(III) complexes were prepared by D. R. Crane by literature methods.¹⁶ The organic quenchers were purchased from Aldrich and recrystallized several times prior to use, typically from acetone. Dichloromethane (Fisher Scientific) and 1,2-dichloroethane (Aldrich) were dried over CaH_2 and distilled under nitrogen prior to use.

Electrochemical Measurements. Electrochemical measurements were carried out at room temperature under argon atmosphere using a Bioanalytical System, INC., Model 100A electrochemical analyzer and a Houston Instrument DMP-40 plotter in the laboratory of Professor W. C. Kaska. Cyclic voltammograms were recorded with a Pt disk working electrode (surface area 0.024 cm^2), a Pt wire counter electrode, and an Ag/AgCl reference electrode. The supporting electrolyte was 0.1 M tetra-*n*-butylammonium hexafluorophosphate (TBAH) in either dichloromethane or 1,2-dichloroethane. The reference electrode was usually separated from the bulk sample solution by a Vycor frit, but in the case of the electrochemical measurements on I, it was further protected from the sample solution with a fritted-glass tube which contained just 0.1 M TBAH in $\text{C}_2\text{H}_4\text{Cl}_2$. Proper IR compensation was made for each measurement, and all $E_{1/2}$ values in this work, determined as $(E_{pa} + E_{pc})/2$, were referenced to the Fc^+/Fc couple, which was independently determined in each solvent. In 1,2-dichloroethane solution (0.1 M TBAH) the CV scan of Fc demonstrated good reversible behavior with peak-to-peak separation of 65 ± 2 mV, and the Fc^+/Fc reduction potential was shown to have a value of 0.47 ± 0.01 V. In dichloromethane $E_{1/2}(\text{Fc}^+/\text{Fc})$ was determined as 0.48 ± 0.02 V. The $E_{1/2}(\text{Q}/\text{Q}^-)$ values for several quenchers were determined by cyclic voltammetry in 0.1 M TBAH/ CH_2Cl_2 , and the results were consistent with the literature values.^{14,17}

Photophysical Measurements. Solutions for Stern-Volmer experiments were prepared as follows. In a volumetric flask Cu_4Ipy_4 and quencher were weighed, and the flask was filled with CH_2Cl_2 to give a solution 0.0100 M in I with the desired concentration of quencher (10^{-4} – 5×10^{-2} M). To these solutions was added a small amount (~ 0.6 mM) of pyridine to inhibit ligand dissociation from the clusters. The solution was transferred to a round pyrex cell (diameter = 0.5 cm) fitted with a greaseless Rotoflow stopcock for anaerobic use and then was degassed by three or four freeze-pump-thaw cycles.

For photophysical measurements at high applied hydrostatic pressure, solutions prepared and deaerated as described above were transferred under N_2 via syringe to a quartz optical capsule capped with a Teflon piston fitted with two Viton O-rings. This capsule was then placed into a Nova Swiss four-window high-pressure spectroscopic cell which was filled with additional solvent as the pressure-transmitting medium. The Nova Swiss cell was attached to an Enerpac hand pump and gauge which were used to generate and measure the applied pressure.

Emission lifetimes were determined as described before¹⁶ with a Quanta-Ray DCR-1A Nd:YAG pulse laser (10 Hz) with an harmonic generator operating at 355 nm (third harmonic) as the excitation source with a laser power of ~ 10 mJ/pulse. The emission was monitored at a right angle to the excitation source using a Schott plastic filter (KV-388) to reduce laser scatter prior to entering a SPEX Model 1680 Doublemate grating monochromator blazed at 500 nm. The emission intensity was monitored at 694 nm with a RCA 8852 PMT. The PMT output was terminated (50 Ω) into a Tektronix 7912AD transient digitizer interfaced to a Zenith Z-158 computer. The signal-averaged data (64 shots per 512-point array) were analyzed by single-exponential curve fitting.

Temperature control of emission samples was obtained with a Haake FK circulating-water bath in the 278–295 K range and a quartz optical Dewar with a CO_2 /ethylene glycol/water bath in the 253–273 K range.

Emission spectra were recorded on Spex Fluorolog2 spectrofluorimeter. Curve-fitting calculations were carried out using KaleidaGraph (version 2.1.3) graphics and curve-fitting software on a Mac IIci computer.

Results

Electrochemical Measurements. The cyclic voltammetry experiments with the Cu_4Ipy_4 cluster proved complicated and suggest that the cluster undergoes reactions in the vicinity of the Pt working electrode. Furthermore, the reproducibility of these cyclic voltammetric experiments depended strongly on the cleanliness of the Pt electrode surface. Nonetheless, these data provide a good, if qualitative, estimate of the ground-state oxidation potential of the cluster I.

The anodic behavior of 1,2-dichloroethane solutions (0.1 M TBAH) of I in the potential range 0 to +1.0 V vs Ag/AgCl qualitatively depends on the scan rate and the concentrations of the cluster and of added pyridine. An anodic scan revealed the presence of two oxidation peaks at $\sim +0.63$ and $\sim +0.80$ V vs Ag/AgCl with corresponding peaks in the cathodic scan at ~ 70 mV less positive potentials in each case ($[\text{I}] \sim 10^{-4}$ M). The number of electrons transferred was not determined, so it is inconclusive whether these represent reversible single-electron processes. Furthermore, since the areas of the peaks observed on the reverse scans are diminished, chemical reactions subsequent to oxidation on a time scale comparable to that of the CV scans are likely. Notably, when the scan rate was increased from 0.05 to 0.5 V s^{-1} , the peak at ~ 0.63 V was suppressed relative to that at the higher anodic potential. Similarly, the former peak was very significantly reduced and the latter increased by the addition of free pyridine (2 mM) to the electrochemistry solution. Thus, it was concluded that the oxidation wave at 0.63 V was the result of a cluster species formed by pyridine dissociation, perhaps a surface reaction on the electrode. The wave at higher potential therefore is concluded to represent oxidation of I. If this is assumed to be a one-electron oxidation, the $E_{1/2}$ value for the I^+/I reduction potential is estimated at 0.77 V vs Ag/AgCl, i.e., 0.30 V vs Fc^+/Fc .

These results are also consistent with CV and Osteryoung square-wave voltammograms (OSWV) performed in dichloromethane solutions (0.1 M TBAH) containing 10 mM cluster and 6 or 31 mM added pyridine. For the higher [py], a single, irreversible anodic peak at 0.75 ± 0.02 V was seen, while at the lower [py], the cyclic wave was more complicated with two anodic peaks at 0.60 and 0.82 V and a cathodic peak at 0.51 V. Similar results were seen in OSWV. Preliminary CV studies using a gold electrode were comparable, a single anodic peak at 0.73 V and a cathodic peak at 0.50 V. Combining these results, the $E_{1/2}(\text{I}^+/\text{I})$ value was estimated at 0.75 ± 0.10 V vs Ag/AgCl, i.e., 0.28 V vs Fc^+/Fc in dichloromethane.

The $E_{1/2}$ values for several organic quenchers were determined by cyclic voltammetry in dichloromethane solutions (0.1 M TBAH). The waves were quasi-reversible ($\Delta E_p = 74$ – 89 mV). The relevant Q/Q^- reduction potentials are summarized in Table I.

Quenching Constants at Ambient Temperature/Pressure. The second-order quenching constants k_q were determined from Stern-Volmer plots.¹⁸ According to eq 2 a plot of τ_0/τ_e vs [Q] for a

$$\tau_0/\tau_e = 1 + k_q\tau_0[\text{Q}] \quad (2)$$

dynamic quenching of I^* should be linear with slope $\tau_0 k_q$, where τ_0 is the lifetime of I in the absence of quencher (3.2 μs) and τ_e is the measured lifetime in the presence of a quencher at concentration [Q]. In a typical experiment (Figure 1), k_q was calculated from a least-squares fit of lifetime measurements made for four different [Q] over an 8-fold range in τ_0/τ_e values. Owing

(16) Crane, D. R.; Ford, P. C. *J. Am. Chem. Soc.* **1991**, *113*, 8510–8516.

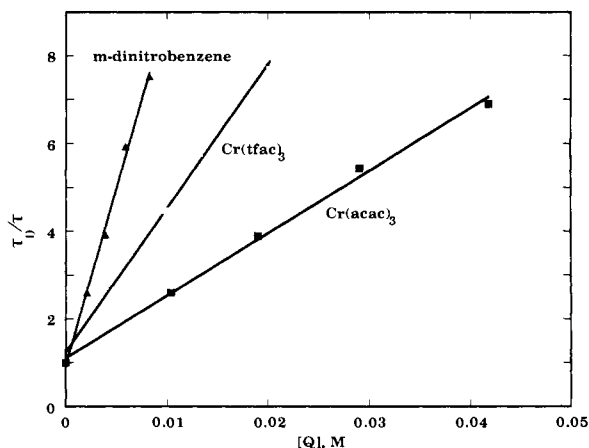
(17) (a) Bock, C. R.; Conner, J. A.; Gutierrez, A. R.; Meyer, T. J.; Whitten, D. G.; Sullivan, B. P.; Nagle, J. K. *J. Am. Chem. Soc.* **1979**, *101*, 4815–4824. (b) Kim, H. B.; Kitamura, N.; Kawnish, Y.; Tazuki, S. *J. Phys. Chem.* **1989**, *93*, 5757–5764.

(18) Turro, N. J. *Modern Molecular Photochemistry*; Benjamin/Cummings: Menlo Park, CA, 1978; pp 243–264.

Table I. Quenching Rate Constants and Activation Parameters for Various Quenchers

quencher ^a	$-E_{1/2}^b$ (V)	$E(^2E_g)^c$ (10^3 cm ⁻¹)	ΔG_{et}^d (V)	$10^{-7}k_q^e$ (M ⁻¹ s ⁻¹)	ΔH^* (kJ mol ⁻¹)	ΔV^* (cm ³ mol ⁻¹)
Cr(acac) ₃	2.43	13.0	0.65 (0.51)	4.7	0.5 ± 0.9	-0.3 ± 0.2
Cr(Br-acac) ₃	1.89 ^f		0.11 (-0.03)	6.9		
Cr(dbm) ₃	1.87	12.1	0.09 (-0.05)	4.6		
Cr(3-SCNacac) ₃	1.66 ^f		-0.12 (-0.26)	11.5		
Cr(tfac) ₃	1.64	12.2	-0.14 (-0.28)	10.9 (7.9) ^g		
Cr(3-NO ₂ acac) ₃	1.57 ^f		-0.21 (-0.35)	7.6		
Cr(tta) ₃	1.43		-0.35 (-0.49)	8.1 (6.2) ^g		
Cr(tfbzac) ₃	1.43	12.3	-0.35 (-0.49)	10.0	0.7 ± 0.2	+0.2 ± 0.2
Cr(hfac) ₃	0.79 (0.78) ^h	12.5	-0.99 (-1.13)	141 (111) ^g	1.1 ± 0.8	+6.6 ± 0.5
<i>m</i> -dinitrobenzene	1.37 (1.34) ^h		-0.41 (-0.55)	0.72 (1.1) ^g	28 ± 1	-8.2 ± 0.4
<i>o</i> -dinitrobenzene	1.26 ^h		-0.52 (-0.66)	0.42	40 ± 2	-7.0 ± 0.9
<i>p</i> -dinitrobenzene	1.18		-0.60 (-0.74)	25.3		
1,4-benzoquinone	0.94 ^h		-0.84 (-0.98)	129	5.4 ± 1.3	+5.2 ± 0.6

^a Ligand abbreviations: acac = 2,4-pentanedionate (acetylacetonate); dbm = 1,3-diphenyl-1,3-propanedionate; hfac = 1,1,1,5,5,5-hexafluoro-2,4-pentanedionate; Br-acac = 3-bromo-2,4-pentanedionate; SCNacac = 3-thiocyanato-2,4-pentanedionate; 3-NO₂acac = 3-nitro-2,4-pentanedionate; tfac = 1,1,1-trifluoro-2,4-pentanedionate; tta = 4,4,4-trifluoro-1-(2-thienyl)-1,3-butanedionate; tfbzac = 4,4,4-trifluoro-1-phenyl-1,3-butanedionate. ^b Reduction potential vs ferrocenium/ferrocene in CH₂Cl₂ (from ref 14). ^c The energy of the Cr(III) ²E_g state (from ref 15). ^d Free energy of the electron-transfer reaction I* + Q = I⁺ + Q⁻, calculated according to eq 4 using the value E_{1/2}(I⁺/I*) = -1.78 V (see text); values in parentheses have the work term -0.14 V added. ^e Second-order quenching constant from Stern-Volmer plots; experimental uncertainties are <±10%. ^f Estimated according to ref 16. ^g The k_q for quenching of the cluster Cu₄I₄L₄, where L = 4-benzylpyridine. ^h This work.

**Figure 1.** Stern-Volmer plots for quenching of LE emission from Cu₄I₄py₄ by different quenchers in CH₂Cl₂ at 297 K.

to absorption by the quenchers at the excitation wavelength (355 nm), a relatively high concentration (10 mM) of I was required.¹⁹ The k_q values and other relevant data for the two series of quenchers are compiled in Table I.

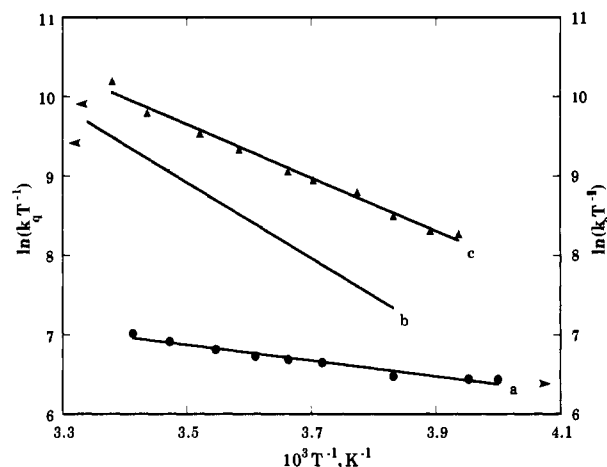
Quenching rates for the excited states of a second tetracopper(I) cluster Cu₄I₄(4-benzylpyridine)₄ (II) were briefly investigated for several quenchers under the same conditions as used for I. The principal emission band for II has a λ_{max} of 694 nm and a τ₀ of 3.7 μs in ambient CH₂Cl₂ solution, only slightly different from those of I*. Notably, the values of k_q proved to be qualitatively very close to those values recorded for the same respective quenchers with I* (Table I).

Temperature effects on the quenching mechanisms were examined over the range 250–297 K. For I in the absence of Q, a plot of ln((1/τ₀)/T) vs 1/T was linear (Figure 2). The slope (-ΔH^{*}/R) was determined via a least-squares fit,²⁰ and the value ΔH^{*} = 8.2 ± 0.5 kJ mol⁻¹ was calculated. For selected quenchers, k_q values were then determined at various T, and activation enthalpies ranging from ~0 to +40 kJ mol⁻¹ were determined (Table I) from the linear plots of ln(k_q/T) vs 1/T for various Q²⁰ (Figure 2).

(19) Although the emission lifetime of the LE ES has been shown (ref 2a) to be independent of [I], the concentration was kept at this value for all the Stern-Volmer experiments described here.

(20) Eyring plots, i.e., $k = (k_B T/h) \exp(\Delta S^*/R) \exp(-\Delta H^*/RT)$.

(21) (a) Ford, P. C. In *Inorganic High Pressure Chemistry. Kinetics and Mechanisms*; van Eldik, R., Ed.; Elsevier: Amsterdam, The Netherlands, 1986; Chapter 6, pp 295–338. (b) van Eldik, R.; Asano, T.; le Noble, W. J. *Chem. Rev.* 1989, 89, 549–688.

**Figure 2.** Plots of ln(k₀/T) and ln(k_q/T) vs T⁻¹ where k₀ = τ₀⁻¹ and τ₀ is the lifetime of the LE ES of Cu₄I₄py₄ without added quencher. Filled circles (a) represent the data without added quencher. Open squares (b) and triangles (c) represent data for the quenchers *m*- and *o*-dinitrobenzene, respectively.

Pressure Effects on Quenching Rates. Hydrostatic pressure effects on quenching rates were examined over the range 0.1–200 MPa at 297 K. The emission lifetime of I* proved to be nearly pressure independent, while k_q values for various Q were, in some cases, much more sensitive to P.

The volume of activation for any dynamic process is defined by²¹

$$\Delta V_i^* = -RT \left(\frac{d(\ln k_i)}{dP} \right)_T \quad (3)$$

where k_i is the rate constant at a particular pressure. This can be determined from the slope (-ΔV_i^{*}/RT) of the ln(k_i) vs P plot at constant T. In the absence of quencher, the ΔV^{*} for the deactivation of I* was found to be -0.6 cm³ mol⁻¹ from the plot of ln(τ₀^a/τ₀) vs P, where τ₀^a is the lifetime at ambient pressure and τ₀ is the lifetime measured at various P. In the presence of selected quenchers, k_q values were determined at different P, and such plots (typically 4–5 points) had the form ln(k_q/k_q^a) vs P, where k_q^a is the value at ambient P and k_q that measured at applied P. These plots were linear within experimental uncertainty for the pressure range investigated (Figure 3). Values of ΔV_q^{*} calculated from the slopes ranged from -8.2 cm³ mol⁻¹ for Q = *m*-dinitrobenzene to +6.6 cm³ mol⁻¹ for Cr(hfac)₃ (Table I).

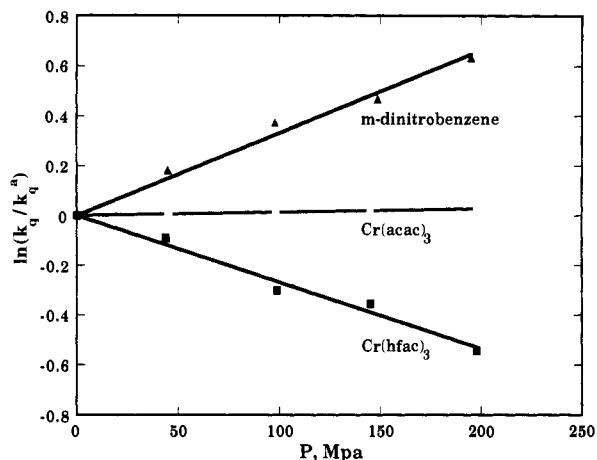


Figure 3. Plots of $\ln(k_q/k_q^0)$ vs pressure for the quenching of the LE ES of Cu_4Ipy_4 by *m*-dinitrobenzene, $\text{Cr}(\text{acac})_3$, and $\text{Cr}(\text{hfac})_3$ in CH_2Cl_2 solution at 297 K.

Discussion

Excited-State Oxidation Potentials. An issue key to the studies described below is the hypothetical half-cell potential for the cluster-centered excited state of Cu_4Ipy_4 , i.e., the $E_{1/2}$ for $\text{I}^+ + e^- \rightarrow \text{I}^*$. This can be estimated by subtracting the calculated ES energy E^{00} from the ground-state reduction potential, i.e.,

$$E_{1/2}(\text{I}^+/\text{I}^*) = E_{1/2}(\text{I}^+/\text{I}) - E^{00} \quad (4)$$

As noted above, the electrochemistry of the cluster **I** is complicated, but CV measurements give an estimate of ~ 0.28 V for $E_{1/2}(\text{I}^+/\text{I})$ vs Fc^+/Fc . The band maxima (691 ± 3 nm, i.e., $1.448 \pm 0.006 \mu\text{m}^{-1}$) and band widths ($0.233 \pm 0.004 \mu\text{m}^{-1}$) of the cluster-centered emission from I^* at room temperature are remarkably constant for different solvents (dichloromethane, toluene, tetrahydrofuran, methyl acetate). The E^{00} value for the CC ES was previously estimated^{2a} as $1.74 \mu\text{m}^{-1}$ (2.16 V) on the basis of the values of the band maxima and band widths and the "1% rule", namely that the E^{00} can be estimated as that frequency where an emission band has an intensity 1% that found at the λ_{max} . For a Gaussian band this can be calculated from the formula $E^{00} = \nu_{\text{max}} + 1.29\nu_{1/2}$, where ν_{max} is the energy of the band maximum and $\nu_{1/2}$ is the full width at half maximum.²² However, recent Franck-Condon analyses here²³ of the shapes of ligand field emission bands have concluded that a "10% rule" might be more appropriate. If so, then E^{00} can be estimated from $E^{00} = \nu_{\text{max}} + 0.91\nu_{1/2} = 1.66 \mu\text{m}^{-1}$ (2.06 V). On the basis of the 1% rule, the calculation $E_{1/2}(\text{I}^+/\text{I}^*) = E_{1/2}(\text{I}^+/\text{I}) - E^{00}$ gives the ES reduction potential as -1.88 V, while this calculation based upon E^{00} estimated according to the 10% rule would give an $E_{1/2}(\text{I}^+/\text{I}^*)$ value of -1.78 V. For the sake of further discussion, the latter, more conservative, value of -1.78 V will be used.

Energy and Electron Transfer. The lowest energy $\pi-\pi^*$ excited states of the nitrobenzenes (2.62 V)^{14,17} and of 1,4-benzoquinone (2.31 V)²⁴ are higher energy than the emitting ES of I^* ; thus energy transfer (eq 1a) would be (at most) a minor quenching pathway. The measured k_q values increase exponentially as the $E_{1/2}(\text{Q}/\text{Q}^-)$ values become less negative, an observation consistent with the expectation that electron transfer (eq 1b) is the dominant quenching mechanism. Each $\text{Cr}(\text{III})$ tris(β -dionato) complex has a low-lying ES (2E) at an energy significantly below that of I^* , so energy transfer is a viable quenching mechanism. The reduction potentials $E_{1/2}(\text{Q}/\text{Q}^-)$ vary over the range -2.43 – 0.79 V (vs Fc^+/Fc in CH_2Cl_2), so that for certain CrL_3 both energy and electron transfer (eq 1) are viable, competitive pathways for

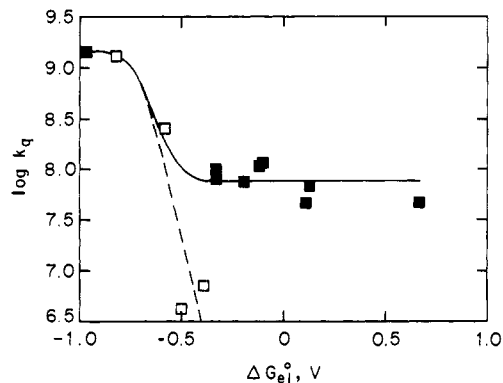


Figure 4. Plot of $\log(k_q)$ vs the free energy of electron transfer ΔG_{el}^0 . Squares and triangles represent experimental data for chromium(III) and organic quenchers, respectively. The dotted and the solid curve represent the least-squares fits to eq 8 as described in text.

quenching I^* , while others will be active only for energy-transfer processes. The energy gap between the I^* donor and the $\text{Cr}(\text{III})$ acceptor is roughly equivalent for all the CrL_3 used; hence rates of energy-transfer quenching should be roughly constant throughout the series.

Figure 4 presents a plot of $\log k_q$ vs ΔG_{el}^0 , where ΔG_{el}^0 is the estimated free energy of the excited-state electron-transfer quenching calculated according to²⁴

$$\Delta G_{\text{el}}^0 = -\{E_{1/2}(\text{Q}/\text{Q}^-) - E_{1/2}(\text{I}^+/\text{I}^*)\} \quad (5)$$

(Actually, the work terms for charge creation $w_p - w_r = -0.14$ V should be added to ΔG_{el}^0).²⁵ This plot indicates three regimes with regard to the quenching rates. At very positive values of ΔG_{el}^0 , electron transfer is not a thermodynamically viable mechanism, yet the CrL_3 quenchers display k_q values between 10^7 and $10^8 \text{ M}^{-1} \text{ s}^{-1}$, reflecting the ability of these species to effect energy-transfer quenching. An example is $\text{Cr}(\text{acac})_3$, which has an $E_{1/2}(\text{Q}/\text{Q}^-) = -2.43$ V (therefore, $\Delta G_{\text{el}}^0 = +0.65$ V), i.e., electron transfer would be strongly endergonic. Nonetheless, $k_q = 4.7 \times 10^7 \text{ M}^{-1} \text{ s}^{-1}$, owing to the exergonic energy transfer, $E(\text{I}^*) - E({}^2E(\text{CrL}_3)) \sim 0.5 \mu\text{m}^{-1}$.

At the other end of the scale, k_q values are much higher at very negative values of ΔG_{el}^0 but seem to level off at $\sim 10^{9.2} \text{ M}^{-1} \text{ s}^{-1}$, somewhat below the value one would expect for a diffusion-limited bimolecular reaction in ambient-temperature CH_2Cl_2 ($\sim 10^{10} \text{ M}^{-1} \text{ s}^{-1}$).²⁶ For example, $\text{Cr}(\text{hfac})_3$ ($E_{1/2}(\text{Q}/\text{Q}^-) = -0.97$), gives a k_q value of $1.4 \times 10^9 \text{ M}^{-1} \text{ s}^{-1}$. The region representing the transition between these extremes seems relatively narrow (several hundred millivolts), although this is partially determined by the limits of the experiment, which cannot measure quenching process with rate constants much less than $10^6 \text{ M}^{-1} \text{ s}^{-1}$. It is notable that the competition between energy- and electron-transfer mechanisms for ES quenching has been shown to be a function of ΔG_{el}^0 for several other luminative metal complexes, examples being $[\text{Cu}(\text{dpp})_2]^{2+}$ quenching by a series of tris(β -dionato)chromium(III) complexes^{14,16} and $[\text{Ru}(\text{bpy})_3]^{2+}$ quenching by ferrocene derivatives.²⁷

Kinetics Model. Scheme I illustrates a model for the processes described above in which it is assumed that quenching involves

(25) (a) For neutral reactants, w_r is zero and $w_p = (Z_+ Z_- e^2 / D_+ d)(1/(1 + \beta d \mu^{1/2})) \sim (Z_+ Z_- e^2 / D_+ d) = -0.14$ V. For calculations here^{25b} $r_D = 7.4 \text{ \AA}$ was estimated for **I** and the average radius $r_Q = 3.8 \text{ \AA}$ was used for the various quenchers.^{17a} (b) Kimura, N.; Kim, H.-B.; Okano, S.; Tazuke, S. *J. Phys. Chem.* **1989**, *93*, 5750–5756. (c) Raston, C. L.; White, A. H. *J. Chem. Soc., Dalton Trans.* **1976**, 2153–2156.

(26) (a) The viscosity of CH_2Cl_2 at 25 °C was estimated from data given at 15 and 30 °C ($\eta \approx 0.41$ cp at 25 °C).^{23b} From the equation^{23c} ($k_d = (2RT/3000\eta)(2 + r_D/r_Q + r_Q/r_D)$) a value of $1.8 \times 10^{10} \text{ M}^{-1} \text{ s}^{-1}$ at 25 °C was calculated. (b) Weast, R. C., Ed. *CRC Handbook of Chemistry and Physics*, 62nd ed.; CRC Press, Inc.: Boca Raton, FL, 1981. (c) von Smoluchowski, M. Z. *Phys. Chem.* **1917**, *92*, 129.

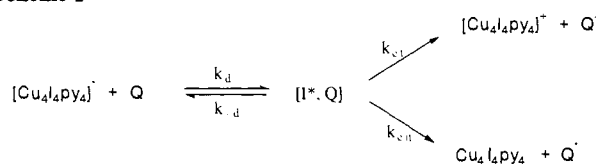
(27) Lee, E. J.; Wrighton, M. S. *J. Am. Chem. Soc.* **1991**, *113*, 8562–8564.

(22) Peterson, J. D.; Watts, R. J.; Ford, P. C. *J. Am. Chem. Soc.* **1976**, *98*, 3188–3194.

(23) McClure, L. J.; Ford, P. C. *J. Phys. Chem.* **1992**, *96*, 6640–6650.

(24) Veenvliet, H.; Wiersma, D. A. *Chem. Phys.* **1975**, *8*, 432–457.

Scheme I



first the diffusion of the two species I^* and Q together to form a precursor complex (P) from which energy and electron transfer are competitive processes. While this is likely to be an oversimplification given that center-to-center distance and orientation requirements of the two mechanisms may be different, the distance requirements for the exchange mechanism for energy transfer should be similar to those for electron transfer. Applying the steady-state approximation to the model described in Scheme I allows one to derive the following expression for the quenching rate constant

$$k_q = \frac{(k_{el} + k_{en})k_d}{k_{-d} + k_{en} + k_{el}} \quad (6)$$

where k_{el} and k_{en} are the unimolecular rate constants for electron and energy transfer (assumed for simplicity to be irreversible), respectively, in the precursor complex (I^* , Q), k_d is the rate constant for diffusion of the two reactants together, and k_{-d} is the rate constant for diffusion of the two components apart before quenching occurs. (A closely analogous situation has been subjected to more rigorous analysis in ref 16.)

For the organic quenchers examined, $k_{el} \gg k_{en}$, and eq 6 simplifies to

$$k_q = \frac{k_{el}k_d}{k_{-d} + k_{el}} \quad (7)$$

One case would be when $k_{el} \gg k_{-d}$, thus $k_q \sim k_d$. In this situation, the second-order quenching rate is limited by the rate of diffusion by the two species in solution. Indeed for the strongly oxidizing quenchers 1,4-benzoquinone and $\text{Cr}(\text{hfac})_3$, k_q has values $\sim 10^{9.2}$ $\text{M}^{-1} \text{s}^{-1}$ approaching the expected diffusion limit ($\sim 10^{10}$ $\text{M}^{-1} \text{s}^{-1}$) for bimolecular quenching in dichloromethane (see below).

A second case would be when electron transfer is the principal quenching mechanism but diffusion apart of the species constituting the precursor complex is much more rapid than electron transfer, i.e., $k_{-d} \gg k_{el}$, thus $k_q \sim k_{el}(k_d/k_{-d})$. For this case, the term k_d/k_{-d} represents the "equilibrium constant" for formation of (I^* , Q),²⁸ and k_q equals the bimolecular rate constant k_{12} for electron transfer between I^* and Q free in solution. The Marcus "cross relation"²⁹ $k_{12} \sim (K_{12}k_{11}k_{22})^{1/2}$ allows one to estimate the relationship between k_{12} , the equilibrium constant K_{12} for electron transfer calculated from the redox potentials,³⁰ and the rate constants k_{11} and k_{22} for self exchange in the systems I^*/I^+ and Q/Q^- , respectively. On the basis of the values of k_{12} and ΔG_{el}° listed in Table I, one can calculate the products $k_{11}k_{22}$ for different quenchers according to the cross relation. For the three dinitrobenzene quenchers, listed values of $k_{11}k_{22}$ fall into the approximate range $10^{6.5 \pm 1.5}$. Values of k_{22} (corrected for solvent effects) have been reported for $\text{Q} = m$ -dinitrobenzene (5.6×10^9 $\text{M}^{-1} \text{s}^{-1}$) and p -dinitrobenzene (6.5×10^9 $\text{M}^{-1} \text{s}^{-1}$).¹⁴ If one (conservatively) assumes an average k_{22} value of 10^9 $\text{M}^{-1} \text{s}^{-1}$ for

(28) From the Fuoss–Eigen equation,^{25b} $k_d/k_{-d} = (4\pi N d^3/3000) \exp(-w_e/RT) \approx 3.5 \text{ M}^{-1}$.

(29) Marcus, R. A. *J. Phys. Chem.* 1968, 72, 891–899.

(30) The calculated ΔG_{el}° is of course very sensitive to the accuracy of the value of $E_{1/2}(\text{I}^*/\text{I}^+)$ (–1.78 V), which is calculated (eq 4) from values of $E_{1/2}(\text{I}^+/\text{I})$, drawn from not fully satisfying electrochemical data, and of E^{00} , conservatively estimated from the emission maximum and band width and the 10% rule (see Discussion). If $E_{1/2}(\text{I}^*/\text{I}^+)$ were less negative, i.e., if the estimate of E^{00} is too high, the over-potential apparently required for efficient electron-transfer quenching would be smaller. However, if one were to make the unlikely assumption that E^{00} occurs at the emission maximum, the shift in ΔG_{el}° would be 0.26 V but not enough to compensate for the over-potential noted here.

such organic oxidants, the cross relation leads to the conclusion that the I^*/I^+ self exchange must be exceedingly slow with an estimated $k_{11} \sim 10^{-2.5}$ $\text{M}^{-1} \text{s}^{-1}$, at the low end of known rate constants for $\text{Cu}(\text{I})/\text{Cu}(\text{II})$ self exchange.³¹ The explanation must lie in the Franck–Condon terms. If there are substantial structural differences between I^* and I^+ , then a slow rate of electron exchange between these species would be expected. Certainly, the very large Stokes shift ($\sim 1.6 \mu\text{m}^{-1}$) between the excitation and emission maxima for I indicates that there is a large distortion between the ground and excited states of the neutral cluster. It is less obvious what would be the structure of the I^+ cation. It is likely that any $\text{Cu}(\text{II})$ character, if localized, would also lead to distortions from the structure of I , but it is equally likely that such distortions are along different coordinates than those resulting from excitation.

A third case, valid only for the CrL_3 quenchers, would be when $k_{en} > k_{el}$ and $k_{-d} > k_{en}$, i.e., the situation when $\Delta G_{el}^\circ > 0$. According to Scheme I, this would give $k_q = k_{en}(k_d/k_{-d})$. Qualitatively, for compounds such as $\text{Cr}(\text{acac})_3$ ($\Delta G_{el}^\circ = +0.65$ V), for which quenching must be by energy transfer exclusively, k_q appears to have a lower limit about $10^{7.6}$ $\text{M}^{-1} \text{s}^{-1}$ in ambient CH_2Cl_2 solutions.

Equation 6 can be rewritten as

$$\frac{1}{k_q} = \frac{1}{k_d} + \frac{1}{k_Q} \quad (8)$$

where $k_Q = (k_d/k_{-d})(k_{el} + k_{en})$. The two curves displayed in Figure 4 were calculated by using the graphics curve-fitting routines to determine the best fit of the k_q values as a function of ΔG_{el}° according to eq 8 and several key assumptions. It was first assumed that the second-order electron transfer part of quenching can be estimated according to the Marcus cross relation, i.e., $(k_d/k_{-d})k_{el} = (k_{11}k_{22}K_{12})^{1/2}$, where $K_{12} = \exp(-\Delta G_{el}^\circ/RT)$. The second was that, for the series of organic quenchers, the second-order energy-transfer component of k_Q is negligible and that, for the CrL_3 series, this has a constant value $(k_d/k_{-d})k_{en}$. (The constancy of energy-transfer rates is an obvious oversimplification although these rates do vary by less than a factor of three.) Calculations were carried out for the organic quenchers using the KaleidaGraph software for curve fitting using k_d and the product $k_{11}k_{22}$ as variables and widely varying initial guesses for these parameters to ensure that the calculated best fit represents global rather than local minima. (This treatment obviously also includes the approximation that k_d and the k_{22} self-exchange constants are roughly the same for each member of the quencher series.) The plot shown for the organic quenchers represents the fit when $k_{11}k_{22} = 10^{6.3 \pm 0.8}$ $\text{M}^{-2} \text{s}^{-2}$ and $k_d = 10^{9.2 \pm 0.7}$ $\text{M}^{-1} \text{s}^{-1}$. The plot shown for the CrL_3 quenchers was calculated using the $k_{11}k_{22}$ and k_d values derived from the organic quenchers, and the best fit so derived gave a $(k_d/k_{-d})k_{en}$ value of $10^{7.9 \pm 0.1}$. However, allowing the curve-fitting routine to vary k_d or $k_{11}k_{22}$ plus k_d led to no significant changes in k_d and only to a modest increase in $k_{11}k_{22}$, but the latter increase was within the uncertainties of these values. Notably, the self-exchange constant for CrL_3 species has been estimated as $\sim 2 \times 10^9$ $\text{M}^{-1} \text{s}^{-1}$, slightly less than those for the dinitrobenzene quenchers, so similar $k_{11}k_{22}$ values for the two series of quenchers would be reasonable.

Two features of these curve fitting results deserve further comment. First, the calculated diffusion limit k_d is about $1/7$ th that one would expect for dichloromethane solution. (The rates of the most reactive quenchers were reexamined by an independent researcher in this lab to confirm the reported result.) One is tempted to speculate on the origin of this result. For example, is this due to an orientation effect, e.g., a requirement the quencher approach I^* only along certain trajectories because close approach to the Cu_4I_4 core is restricted along most trajectories owing to

(31) Knapp, S.; Kennan, T. P.; Zhang, X.; Fikar, R.; Potenza, J. A.; Schugar, H. J. *J. Am. Chem. Soc.* 1990, 112, 3452–3464.

the bulk of the pyridines coordinated to each Cu? The second point is the very low value of the estimated $k_{11}k_{22}$, $10^{6.3\pm 0.8} \text{ M}^{-2} \text{ s}^{-2}$. Although the self-exchange constants k_{22} would certainly vary from one quencher to another, it appears that each Q utilized in the present study would have values $>10^9 \text{ M}^{-1} \text{ s}^{-1}$; thus, as noted above, the I^*/I^+ self-exchange constant k_{11} must have a very small value, $<10^{-2} \text{ M}^{-1} \text{ s}^{-1}$, the logical explanation being large reorganization energy terms (see below).

Temperature and Pressure Effects. From Table I it is seen that the three regimes of the plot in Figure 4 are also reflected in the temperature and pressure effects on k_q . In the region where $\Delta G_{\text{el}}^\circ$ is positive and the quenching by CrL_3 must be dominated by the energy-transfer mechanism, e.g., for $\text{Q} = \text{Cr}(\text{acac})_3$, the enthalpy of activation ΔH_q^\ddagger and volume of activation ΔV_q^\ddagger are both very small, $\sim 0 \text{ kJ mol}^{-1}$ and $\sim 0 \text{ cm}^{-3} \text{ mol}^{-1}$, respectively. In energy transfer, no net charge is transferred; thus the solvent reorganizational energy is minimal. At the other extreme, where $\Delta G_{\text{el}}^\circ$ is large and negative, the quenching mechanism appears to be dominated by a near-diffusion-limited electron-transfer process, i.e., $k_q \sim k_d$. In these cases, the temperature and pressure effects would reflect the response of k_d to these parameters, especially solvent viscosity. Consistent with this are the results for $\text{Q} = \text{benzoquinone}$ ($k_q = 1.3 \times 10^9 \text{ M}^{-1} \text{ s}^{-1}$) and $\text{Cr}(\text{hfac})_3$ ($1.4 \times 10^9 \text{ M}^{-1} \text{ s}^{-1}$); the activation enthalpy ΔH_q^\ddagger is quite small ($+5.4$ and 1.1 kJ mol^{-1} , respectively) while the significantly positive values for ΔV_q^\ddagger ($+5.2$ and $+6.6 \text{ cm}^{-3} \text{ mol}^{-1}$, respectively) reflect the increased viscosity as hydrostatic pressure increases. Notably, the diffusion controlled quenching of $[\text{Cu}(\text{dpp})_2]^{2+}$ by $\text{Cr}(\text{hfac})_3$ ($9.4 \times 10^9 \text{ M}^{-1} \text{ s}^{-1}$) and *p*-dinitrobenzene ($10.5 \times 10^9 \text{ M}^{-1} \text{ s}^{-1}$) in dichloromethane displayed ΔV_q^\ddagger values of $+8.0$ and $+6.9 \text{ cm}^{-3} \text{ mol}^{-1}$, respectively.¹⁶

The most interesting activation parameters are those recorded for electron-transfer quenching of I^* by *m*-dinitrobenzene ($k_q = 7.2 \times 10^6 \text{ M}^{-1} \text{ s}^{-1}$) and by *o*-dinitrobenzene ($4.2 \times 10^6 \text{ M}^{-1} \text{ s}^{-1}$), for which $k_q \ll k_d$. For these two systems, ΔV_q^\ddagger was found to be large and negative, -8.2 and $-7.0 \text{ cm}^{-3} \text{ mol}^{-1}$, respectively.^{32,33} Such a negative value of ΔV_q^\ddagger would be the consequence of solvent electrostriction in the transition state for electron transfer, i.e.,

(32) (a) The observed volume of activation ΔV_q^\ddagger can be written^{31b} as $\Delta V_q^\ddagger = \Delta V_{\text{in}}^\ddagger + \Delta V_{\text{os}}^\ddagger + \Delta V_{\text{Coul}}^\ddagger + \Delta V_{\text{DH}}^\ddagger$, where $\Delta V_{\text{in}}^\ddagger$ represent the inner sphere reorganization (in), outer sphere reorganization (os), Coulombic work (Coul), and work from ionic strength (Debye-Hückel) effects (DH), respectively. For neutral reactants, $\Delta V_{\text{Coul}}^\ddagger$ and $\Delta V_{\text{DH}}^\ddagger$ would be zero. $\Delta V_{\text{os}}^\ddagger$ can be calculated by (1) the Stranks-Hush-Marcus model (SHM),^{32b,c}

$$\Delta V_{\text{os}}^\ddagger(\text{SHM}) = (\text{Ne}^2/16\pi\epsilon_0) \left\{ (1/2r_{\text{D}} + 1/r_{\text{Q}} - 1/d) \left\{ \partial/\partial p (1/n^2 - 1/\epsilon_s) \right\}_T - (1/n^2 - 1/\epsilon_s) \beta/3d \right\}$$

or (2) Cannon's model,^{33b}

$$\Delta V_{\text{os}}^\ddagger(\text{ell}) = [\text{Ne}^2 d^2 S(\lambda_0) / \{16\pi\epsilon_0 b^2 (2b + d)\}] \left\{ \partial/\partial p (1/n^2 - 1/\epsilon_s) \right\}_T - \{e^2 d^2 S(\lambda_0) (d + 4b) / \{48\pi\epsilon_0 b^2 (2b + d)\} (1/n^2 - 1/\epsilon_s) \beta$$

where geometric factor $S(\lambda_0) \approx 0.82$ with major radius $a = 11.2 \text{ \AA}$ and minor radius $b = 6.41 \text{ \AA}$ for the ellipsoidal model. All other notations have the conventional meanings and can be numerically estimated from the tabulations^{32a,d} and experimental data.^{31e} At 100 MPa in CH_2Cl_2 , $\Delta V_{\text{os}}^\ddagger(\text{SHM})$ and $\Delta V_{\text{os}}^\ddagger(\text{ell})$ are -6.0 and $-7.4 \text{ cm}^{-3} \text{ mol}^{-1}$, respectively. (b) Swaddle, T. W. In *Inorganic High Pressure Chemistry*; van Eldik, R., Ed.; 1986; pp 273-294. (c) Swaddle, T. W. *Inorg. Chem.* 1990, 29, 5017-5025. (d) Isaacs, N. S. *Liquid Phase High Pressure Chemistry*; J. Wiley and Sons: New York, 1981; Chapter 2. (e) Diquet, R.; Deul, R.; Franck, E. U. *Ber. Busen-Ges. Phys. Chem.* 1983, 89, 800-804.

the collapse of solvent around the dipole created as an electron is passed from I^* to Q. Accompanying this process may be changes in the inner sphere coordinates, although it is not clear whether these should be positive or negative. Ab initio calculations suggest that excitation of I to I^* leads to increased Cu-Cu bonding but decreased Cu-I bonding;^{2d} hence the volume differences between ground and excited state are likely to be small given the very small pressure effect on the unquenched decay of I^* ($0.6 \text{ cm}^3 \text{ mol}^{-1}$). On the other hand, the large inner sphere Franck-Condon effects are suggested by the very small estimated value for the I^*/I^+ self-exchange rate and solvent electrostriction is indicated by the negative ΔV_q^\ddagger values. Thus, the significantly positive ΔH^\ddagger values ($+28$ and $+40 \text{ kJ mol}^{-1}$, respectively) found even for these relatively fast electron-transfer reactions ($k_q > 10^6 \text{ M}^{-1} \text{ s}^{-1}$) may be attributed to this combination of inner and outer sphere reorganization energies.³³ Electron-transfer rates should maximize when the reaction driving force ($-\Delta G_{\text{el}}^\circ$) approaches the total inner and outer sphere reorganization energy λ .³³ Thus, the very negative $\Delta G_{\text{el}}^\circ$ values required before k_q approaches the diffusion limit clearly indicates substantial contribution from the inner sphere contribution λ_{in} as well as from the outer sphere solvent rearrangement λ_{os} .³³

An interesting comparison can be made between the results for quenching by *m*- and *o*-dinitrobenzenes and by $\text{Cr}(\text{tfzac})_3$. Although the calculated $\Delta G_{\text{el}}^\circ$ for electron transfer is about 60 mV less favorable for $\text{Cr}(\text{tfzac})_3$ than for *m*-dinitrobenzene, the former is about an order of magnitude more effective in quenching I^* . However, the activation parameters for the $\text{Cr}(\text{III})$ complex (especially the $\Delta V_q^\ddagger \sim 0$) clearly point to energy transfer as the principal quenching mechanism in the latter case.

Summary. The qualitative behavior of this system is similar to that of the $[\text{Cu}(\text{dpp})_2]^{2+}/\text{CrL}_3$ system studied previously.³ However, from Figure 4 it is seen that, for the $\text{Cr}(\text{III})$ quenchers, electron transfer from I^* becomes a competitive quenching pathway and k_q for the organic quenchers becomes measurable ($>10^6 \text{ M}^{-1} \text{ s}^{-1}$) when $\Delta G_{\text{el}}^\circ$ approaches -0.5 V (or $\sim -0.6 \text{ V}$ if the work terms are included)³⁰ in contrast to the $[\text{Cu}(\text{dpp})_2]^{2+}$ system, where electron-transfer quenching was found to become competitive at $\sim +0.2 \text{ V}$. This difference cannot be explained in terms of solvent reorganizational energies alone. The self-exchange rate constant for $[\text{Cu}(\text{dpp})_2]^{2+}/[\text{Cu}(\text{dpp})_2]^{2+}$ has been estimated to be $\sim 10^9 \text{ M}^{-1} \text{ s}^{-1}$, consistent with the ES in that system being a MLCT with Cu already formally in the 2+ oxidation state. In contrast, a large inner sphere reorganization energy must accompany the oxidation of the cluster-centered XMCT/d-s excited state I^* . This is reflected by the very small calculated self-exchange rate constant for the $[\text{Cu}_4\text{I}_4\text{py}_4]^{2+}/[\text{Cu}_4\text{I}_4\text{py}_4]^{2+}$ couple and the surprisingly large activation enthalpies (0.3 - 0.4 V) seen for those systems where electron transfer is apparently the sole or principal quenching mechanism but the rates are not diffusion limited.

Acknowledgment. This research was supported by a National Science Foundation grant to P.C.F. (CHE90-24845) and a Danish Natural Sciences Research Council grant to A.D. (11-8793).

(33) (a) According to Marcus-Hush theory,¹⁷ $\Delta G_{\text{el}}^\ddagger = \lambda/4(1 + \Delta G_{\text{el}}^\circ/\lambda)^2$, where $\lambda = \lambda_{\text{in}} + \lambda_{\text{os}}$. The outer sphere reorganization energy λ_{os} was estimated from the spherical and ellipsoidal models^{33b,c} as $\sim 0.6 \text{ V}$. (b) Cannon, R. D. *Chem. Phys. Lett.* 1977, 49, 299-304. (c) Brunschwig, B. S.; Ehrenson, S.; Sutin, N. *J. Phys. Chem.* 1986, 90, 3657-3668.